53rd International Conference on Environmental Systems
21-25 July 2024, Louisville, Kentucky

ICES-2024-156

Integrated Simulations of the Sabatier and Carbon Vapor Deposition Reactor to Understand Its Impacts to Operations and Performance

Thomas T. Chen[1]
NASA Johnson Space Center, Houston, TX, 77058, USA

The carbon vapor deposition (CVD) reactor is a technology developed by Honeywell Aerospace to convert methane, at high temperatures, into hydrogen and solid carbon. This element is coupled with a Sabatier reactor to support a closed-loop environmental control and life support system with the aim of achieving nearly complete oxygen recovery (> 95%). Initial open-loop, brassboard CVD reactor tests and simulations have shown the CVD's ability to achieve moderately high methane conversion and high hydrogen selectivity. However, in an integrated system, additional deficiencies are expected due to recycling of unreacted or extraneous species from the Sabatier reactor (e.g., carbon dioxide, hydrogen, water) and CVD reactor (e.g., hydrocarbons, methane, etc.). Sabatier and CVD reactor models were integrated and simulated to predict potential impacts to individual reactors' and the overall system's performance. The simulations showed that increasing the recycle of the CVD effluent hydrogen combined with decreasing the system inlet hydrogen flow rate (i.e., drawing a stoichiometric flow rate from an electrolyzer) can lead to an oxygen recovery of > 95%. However, system integration comes at a detriment to the individual reactors. The simulations show the initial conversion from the integrated system (Sabatier = 87% and CVD = 59%) to be lower than the standalone systems (Sabatier = 91% and CVD = 69%). Furthermore, transient simulations show substrate densification, leading to worsening methane conversion coupled with increasing acetylene production, which is commensurate with soot formation. Simulations predict a shortening of the maintenance interval (i.e., time until CVD methane conversion drops below 50%) in the integrated system, which would increase the consumable substrate mass. These analyses highlight the importance of long-duration, integrated tests to corroborate these findings as well as suggest potential modifications (e.g., intermediate gas separations) to improve performance.

Nomenclature

ACM	=	Aspen Custom Modeler
CDRA	=	carbon dioxide removal assembly
CDRS	=	carbon dioxide removal system
CH_4	=	methane
C_2H_2	=	acetylene
C_6H_6	=	benzene
CM	=	crewmember
CO_2	=	carbon dioxide
CVD	=	carbon vapor deposition
ECLSS	=	environmental control and life support system
FBCO2	=	4-bed carbon dioxide scrubber
GC	=	gas chromatography
GIEM	=	Gateway Integrated ECLSS Model
H_2	=	hydrogen
H_2:CO_2	=	hydrogen-to-carbon-dioxide ratio
H_2O	=	water
ISS	=	International Space Station
OGA	=	oxygen generation assembly
PCI	=	Precision Combustion, Inc.
SA	=	Sabatier assembly
SDU	=	Sabatier development unit
X_{CH4}	=	methane conversion

[1] ECLSS Analyst, Crew & Thermal Systems Division, NASA JSC.

I. Introduction

In consideration of the closed-loop environmental control and life support system (ECLSS) to facilitate long-duration human exploration, spacecraft life support technologies, such as a Sabatier[1-5] and carbon vapor deposition (CVD) reactor system[6-9] have been developed and we have demonstrated the capability of each individual system to provide sufficient function to recycle and transform the prevalent metabolic gas product carbon dioxide (CO_2) into breathing oxygen (O_2).

Figure 1 shows a notional closed-loop ECLSS architecture. CO_2 is collected and concentrated by a CO_2 removal system, such as the carbon dioxide removal assembly (CDRA)[10,11] or 4-bed carbon dioxide scrubber (FBCO2).[12-15] The accumulated CO_2 is then delivered in conjunction with hydrogen (H_2), which is produced by the oxygen generation assembly (OGA), to a CO_2 reduction system (i.e., Sabatier reactor) to convert the CO_2 into water (H_2O) and byproduct methane (CH_4). Various Sabatier-based CO_2 reduction technologies have been developed. The Sabatier assembly had been operated on the International Space Station from 2011 to 2017 until recent return and upgrades to support improved reliability and stability for exploration.[1-3] Another Sabatier system was developed by Precision Combustion, Inc. (PCI)[4,5]. PCI's Sabatier development unit (SDU) utilizes their Microlith® catalytic technology to produce a compact Sabatier reactor system that is able to achieve high CO_2 conversion and CH_4 selectivity at high space velocities.

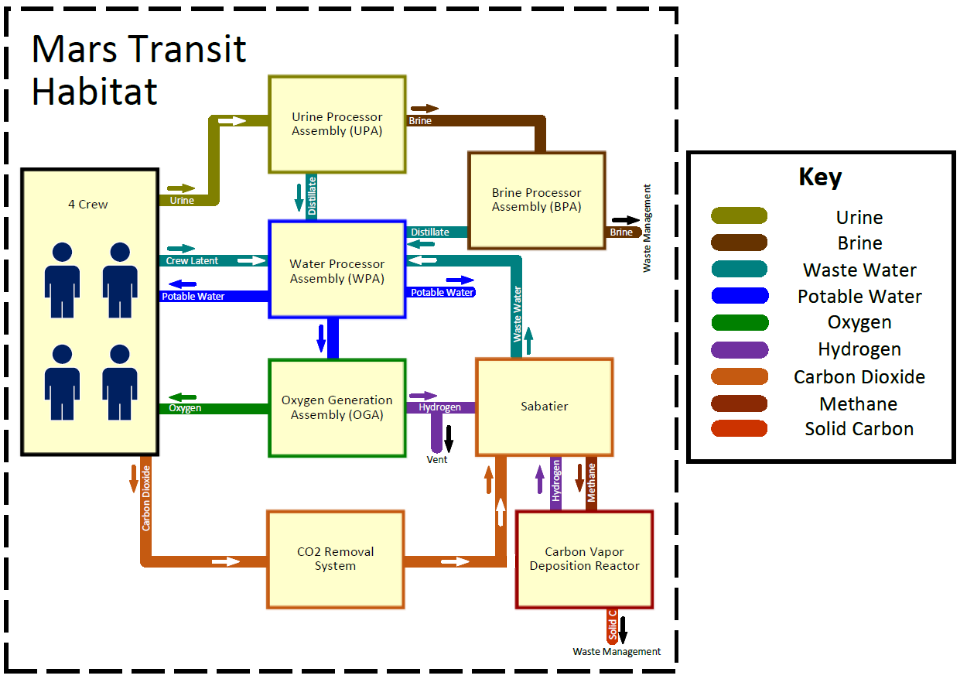

Figure 1. Notional closed-loop ECLSS architecture with CO_2 reduction.

The Sabatier reaction (as shown in Equation 1) produces H_2O from CO_2, which is inevitably delivered to the OGA to regenerate O_2. However, its byproduct CH_4 was vented as part of the International Space Station Air String demonstration with the Sabatier assembly[16]. This loss of H_2 in the form of CH_4 limits the ECLSS's maximum O_2 recovery to 50%.

$$CO_2 + 4\,H_2 \rightleftharpoons CH_4 + 2\,H_2O \qquad \text{Equation 1}$$

Processing and recovering H_2 from CH_4, hence, becomes pertinent to fully closing the spacecraft O_2 balance when using a Sabatier-based ECLSS system. The CVD (or CH_4 pyrolysis) reactor developed by Honeywell is one such technology for closing the air loop to enable near 100% O_2 recovery.[6-9] As shown in Figure 1, the CVD reactor system takes in CH_4 and produces H_2 and solid carbon (C(s)), where the former may be used to supplement the requisite H_2 needs of the Sabatier reactor. The CVD reactor uses the non-oxidative thermal decomposition of CH_4 at high temperatures (i.e., > 1,000 °C), also known as CH_4 pyrolysis, to produce H_2, C(s), and other carbonaceous species. The CVD reactor uses a carbon fiber substrate within its reactor volume to immobilize solid pyrolytic carbon rather than allowing the formation of soot entrained in the process gas flow. This simplifies the separations and cleanup of the process gases. Honeywell's brassboard CVD reactor has demonstrated the ability to convert 4 crewmembers (CMs) worth of CH_4 with reasonably high conversion (50 – 80%) and high H_2 selectivity (> 95%).

To assess these CO_2 reduction systems (i.e., Sabatier and CVD reactor) under more realistic operational scenarios, integrated testing is needed to elucidate the effects of integration, recycling of byproducts, incomplete conversion, and imperfect selectivity. By leveraging existing models of the individual Sabatier and CVD reactors,[17] a model of the integrated system may be developed to perform predictive performance assessments closer to their real operational state. The integrated model may then be used to provide a priori insights into the expected behavior to inform integrated test development. Integrated modeling and simulation is powerful in that the models are more flexible compared to real hardware to account for different test configurations; they allow for rapid analysis of different operating conditions; running the simulations requires fewer resources compared to hardware integration and testing; and the models provide detailed tracking of all process parameters (e.g., compositions and flow rates) that may otherwise be cumbersome to acquire in testing. The objective of this integrated modeling and simulation effort for the combined Sabatier and CVD reactor systems is to provide a priori predictions on the effects of integration (e.g., recycling of byproducts, incomplete conversion, etc.) on the individual reactor and overall system performances.

II. Integrated Model Formulation

A. Sabatier Reactor Model Description

The Sabatier reactor model used for this integrated modeling effort was based on PCI's SDU, which was delivered to NASA as part of Contract NNX11CC05CSDU.[4,5] The SDU includes the Sabatier reactor portion, which was modeled as a plug flow reactor due to its high operating space velocities, and a H_2O condenser, which is modeled as a vapor liquid equilibrium at a fixed outlet setpoint temperature. To keep the model simple but insightful, the SDU model solely includes the major reactions of CO_2 methanation (Equation 1), CO methanation (Equation 2), and the reverse water gas shift reactions (Equation 3).

$$CO + 3\,H_2 \rightleftharpoons CH_4 + H_2O \qquad \text{Equation 2}$$

$$CO_2 + 2\,H_2 \rightleftharpoons CO + H_2O \qquad \text{Equation 3}$$

The kinetic parameters for these reactions were fitted using test data of the CO_2 conversion and CH_4 selectivity at different steady-state conditions (55 combinations of temperature, pressure, and hydrogen-to-carbon-dioxide ratio [H_2:CO_2]) as well as time-resolved gas chromatography (GC) data. Over the steady-state test points, the model was able to predict CO_2 conversion with an average error of ± 2.8% and standard deviation of 1.9%. The time-resolved GC data was able to be simulated with an average error on the mole percent of CO_2, H_2, CH_4, and carbon monoxide of ± 3.2 mol%, ± 4.0 mol%, ± 5.5%, and ± 0.3%, respectively. The model is able to achieve good agreement with the test data.

B. Carbon Vapor Deposition Reactor Model Description

A CVD reactor model was developed to capture the multitude of physicochemical phenomena that constitute this highly dynamic system.[17] The model considers the homogeneous gas-phase CH_4 pyrolysis reactions, the heterogeneous solid carbon deposition and substrate densification phenomenon, and the axial gas transport through the reactor volume and its multiple carbon fiber substrate layers. The 1-D CVD reactor model material balance was based on a general packed-bed, axial dispersion plug flow reactor model, and the original kinetic model included the consideration of 59 different gaseous and surface species and 243 total reactions. Based on the sensitivity analysis over the entire reaction network as described in Chen, *et al.* (2024), the most insensitive reactions were removed from the model to improve model run times while maintaining nearly equivalent model results. The reaction network for the CVD reactor model was reduced from 243 reactions to 136 reactions, which led to a marked reduction in computational run times and improved model stability.

C. Integrated SDU and CVD Reactor Model Description

Both the SDU and CVD reactor models were developed using Aspen Custom Modeler (ACM) due to its ability to allow for custom model development while leveraging its ordinary and partial differential equation solvers as well as Aspen's large chemical properties database. The ACM software also allows already built models to be readily connected to simulate integrated systems and processes. An example of such a model is the Gateway Integrated ECLSS Model (GIEM) that includes various subsystems of the Gateway air revitalization system such as the CO_2 and humidity control, CO_2 removal system, condensing heat exchanger, and more.[18] The SDU and CVD reactor models were integrated by connecting the SDU gas outlet to the CVD reactor model's inlet and recycling the CVD gas outlet to the SDU inlet to close the loop. The integrated models are shown in Figure 2.

Some key features of the integrated model are noted. Firstly, the integrated system assumes no intermediate H_2 separations between the CVD reactor and the SDU inlet, where all the CVD effluent may be directed to recycle to the SDU. If a viable H_2 separator for spacecrafts exists, the model may be updated to reflect that unit process. Additionally, the SDU was designed for a 3.24 crewmember (CM) processing rate, whereas the CVD reactor was designed to be able to process a 4 CM load. Therefore, the integrated model includes scale-up and scale-down process units that can be used to arbitrarily increase the total molar flow while maintaining the same composition. This illustrates one of the strengths of modeling, where it is easily adjustable compared to hardware testing, which would involve more complex gas supplement and purge designs, flow controller selection and calibration, and potentially in-line gas analyzers to determine instantaneous gas effluent compositions. The integrated SDU and CVD reactor model contains a process unit called a stream splitter, which is used to adjust the ratio of recycle flow rate of CVD reactor gas effluent back to the SDU versus the portion that is purged. Real-world chemical process systems that employ a recycle stream will typically purge a portion of the reactor effluent out of the process to prevent buildup of undesirable products that may dilute the reactants and limit system performance. The integrated SDU and CVD reactor model will be used to assess different recycle and purge flow rates to determine their effect on performance (i.e., individual reactor conversion and system O_2 recovery).

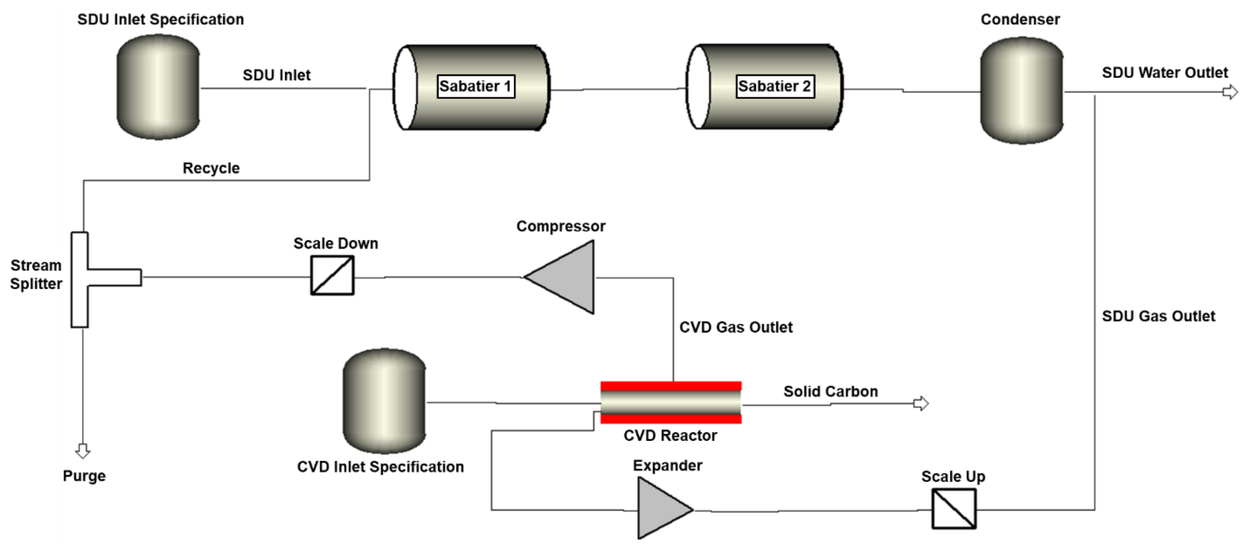

Figure 2. Depiction of the integrated SDU and CVD reactor models in ACM.

III. Integrated Model Assumptions

To perform the integrated modeling and simulation of the combined SDU and CVD reactor system, the set of operating conditions that define the individual subsystem's nominal operations is established. **Table 1** lists the nominal operating conditions for the standalone SDU and CVD reactor systems. However, under integrated system operations, these values will likely deviate from the nominal values due to incomplete conversion and imperfect selectivity that will result in the recycling of unreacted reactants (e.g., CO_2 and CH_4) and byproducts (e.g., acetylene [C_2H_2]). Additionally, due to the dynamic nature of the CVD reactor, whose substrate fills with solid carbon over time, the real operations of the integrated system will also be dynamic with worsening CH_4 conversion in the CVD reactor over time and hence less H_2 being recycled back to the SDU. This integrated model has not implemented any feedback control mechanism to adjust the H_2 flow over the course of a run to maintain a specific H_2:CO_2 but rather recycles a specified fraction of the CVD reactor effluent, whose composition will inherently change over time. The simulation results may be informative as to whether a more sophisticated flow control scheme will be necessary.

Table 1. SDU and CVD Reactor Nominal Operating Conditions

Operating Parameters	Nominal Values
Sabatier Reactor	
CO_2 Feed Rate	1.3 SLPM (or 3.24 CM equivalent)
H_2:CO_2	4, 4.25, 4.5
Average Reactor Temperature	~350 °C
CVD Reactor	
CH_4 Feed Rate	1.6 SLPM (or 4 CM equivalent)
Setpoint Temperature	1170 °C

IV. Integrated SDU and CVD Reactor Model Results

The integrated SDU and CVD reactor model is useful for providing predictions on the overall system performance versus trying to justify system capabilities based solely on operation of the standalone systems. The integrated model may also help to provide input into integrated system test planning. The use of models to perform this type of integrated analysis leverages existing models of the two subsystems (i.e., the SDU and CVD reactor) and may be performed over a wide array of conditions with less resource overhead compared to hardware integration and testing.

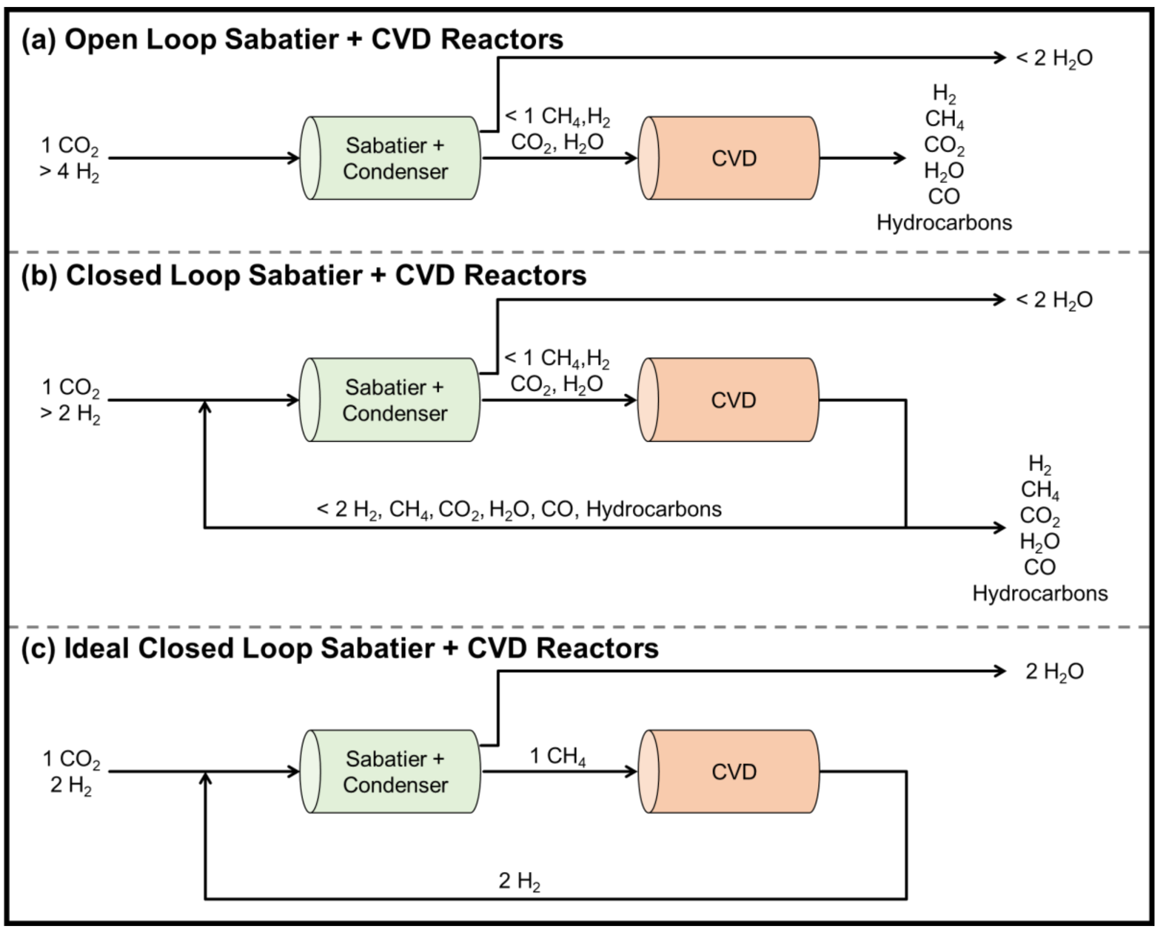

Figure 3. Examples of the integrated Sabatier + CVD reactors configurations.

Figure 3 depicts some of the scenarios that were simulated using the integrated SDU and CVD reactor model. The open-loop Sabatier and CVD reactors (Figure 3a) shows how, without recycling any of the H_2 derived from CH_4, the system's O_2 recovery is limited to a maximum of 50% where the H_2O produced by the system carries half of the H_2 that was fed into the system. In an ideal system (Figure 3c), both the Sabatier and CVD reactors operate at 100% conversion and 100% product selectivity to entirely close the O_2 balance (i.e., 100% O_2 recovery). The ideal system is able to reduce CO_2 using H_2 into H_2O and C(s) according to their stoichiometric ratios (i.e., 1 CO_2 + 2 H_2O → C (s) + 2 H_2O) without any gaseous byproduct formation and a solid carbon waste. In reality, both the Sabatier and CVD reactors operate at < 100% conversion and < 100% selectivity, so a situation like that shown in Figure 3b is expected. Due to recycling of the CVD reactor effluent, the integrated system's O_2 recovery may be markedly improved over an ECLSS with only a Sabatier reactor or the open-loop system (Figure 3a). However, incomplete conversion and imperfect selectivity may inherently limit the O_2 recovery to < 100%.

The integrated SDU and CVD reactor model was used to assess the following cases: (1) steady-state open-loop integration with no recycle, (2) steady-state closed-loop integration, and (3) transient closed-loop integration. The steady-state open-loop integrated system is used to represent the baseline effect of a pure SDU effluent feed to the CVD reactor. The closed-loop integrations are used to provide insight into how recycling the CVD reactor effluent affects the overall system performance and necessary maintenance interval (i.e., time between substrate changeouts).

A. Open-loop Integration and Baseline Results

The integrated SDU and CVD reactor was simulated in an open-loop configuration to establish the baseline effect of a pure SDU effluent on the downstream CVD reactor. The system was assessed with a H_2:CO_2 of 4, 4.25, and 4.5. According to the Sabatier reaction stoichiometry (Equation 1), a H_2:CO_2 of 4 is necessary if 100% conversion were achieved. However, the reaction thermodynamics will limit the maximal equilibrium conversion of CO_2 and H_2 to CH_4 and H_2O. Therefore, it is common to operate the Sabatier reactor with an excess amount of H_2 to shift the equilibrium toward the products according to Le Chatelier's principle.

Table 2. Open-loop Integration Simulation Results

	H_2:CO_2		
	4	**4.25**	**4.5**
Operating Parameter			
SDU Inlet Flow Rate	15.95 mol/hr	16.75 mol/hr	17.55 mol/hr
SDU Inlet Composition	20.0% CO_2 80.0% H_2	19.0% CO_2 81.0% H_2	18.2% CO_2 81.8% H_2
Performance Parameter			
H_2O Production Rate	5.50 mol/hr	5.70 mol/hr	5.84 mol/hr
SDU Conversion	90.5%	93.8%	96.3%
CVD Reactor Conversion	69.5%	67.7%	65.4%
SDU O_2 Recovery	86.2%	89.3%	91.6%
System O_2 Recovery	43.1%	42.0%	40.7%

The results from the open-loop integrated simulation are shown in **Table 2**. The SDU results show the reactor to operate with > 90% conversion, which increases with H_2:CO_2. Similarly, the SDU O_2 recovery increases from 86.2% to 91.6% with an increase in the H_2:CO_2 from 4 to 4.5. However, feeding an SDU gas effluent into the CVD reactor does appear to lead to a detriment in performance. Due to H_2 inhibition and dilution effects, the CVD reactor conversion worsens with increasing H_2:CO_2. These open-loop simulations already show how integration of the individual systems can lead to a difference in performance level of the integrated system compared to what may be expected based on solely standalone testing.

The system O_2 recovery is determined by the H_2O condensed from the SDU divided by the larger of either the O_2 or H_2 fed into the integrated system (Equation 4). The CVD reactor gas effluent in the open-loop configuration is assumed to be vented. Therefore, the system O_2 recovery tends to be dictated by the recovery of H_2. Therefore, although the SDU O_2 recovery is high, the system O_2 recovery is significantly lower and even decreases from 43.1%

to 40.7% when the H_2:CO_2 is increased from 4 to 4.5. The reason is that additional H_2 is being fed into the system for marginally more H_2O production. This is an interesting insight that appears to subvert the logic that improving the Sabatier reactor's conversion is beneficial for the entire spacecraft when in reality it may be disadvantageous.

$$\text{System } O_2 \text{ Recovery} = \frac{\text{SDU } H_2O \text{ Product}}{\max(O_2 \text{ or } H_2 \text{ feed})} \qquad \text{Equation 4}$$

These initial open-loop simulations define the baseline conversions and recoveries that the closed-loop system will be compared against.

B. Closed-loop Integration Results

The integrated SDU and CVD reactor was simulated in a closed-loop configuration with different recycle flow rates to determine how recycling the CVD effluent would incrementally affect the individual reactor and integrated system performances. Two types of simulations were performed: steady-state simulations with a fresh substrate (i.e., without carbon deposition) and transient simulations with a dynamic substrate (i.e., with carbon deposition).

1. Fresh Substrate Simulation Results

Steady-state simulations with a fresh substrate were performed with recycle flow rates of approximately 5 – 70 mol/hr and system inlet H_2:CO_2 of 2.03 – 3.00. This represents an integrated system with partial recycle of the CVD effluent to nearly complete loop closure. The closer the system is to full loop closure, the greater the recycle flow rates become and the lower the system inlet H_2:CO_2 can be to sustain the Sabatier reaction. Figure 4 shows plots of the mixture H_2:CO_2 (Figure 4a), Sabatier conversion (Figure 4b), and CVD conversion (Figure 4c) at different recycle flow rates and system inlet H_2:CO_2. The green box in the plots bounds the SDU inlet H_2:CO_2 between 4 and 4.5, which is its nominal operating range during standalone SDU testing. Figure 4b and Figure 4c also show the baseline Sabatier and CVD reactor conversions from the open-loop simulations at a H_2:CO_2 of 4, 4.25, and 4.5 as points of comparison. Figure 4 is used to describe the effect of the CVD effluent recycle on the individual reactor performance.

The mixture H_2:CO_2 represents the inlet into the SDU after the system feed is mixed with the recycled CVD effluent. As shown in Figure 4a, the mixture H_2:CO_2 increases with the recycle flow rate at a constant system inlet H_2:CO_2. It makes sense that, as you recycle more of the CVD effluent, which is predominantly H_2, the H_2:CO_2 going into the SDU will also increase. Another way to read Figure 4a is that, as the recycle flow rate increases, the system is able to operate with a lower system inlet H_2:CO_2 (i.e., lower H_2 feed into the system) while maintaining the requisite stoichiometry for the Sabatier reaction (i.e., minimum of 4 H_2 to 1 CO_2). The goal is to achieve a system inlet H_2:CO_2 of 2:1, which mimics the generation of H_2 and O_2 from water electrolysis and would result in 100% O_2 recovery.

However, as shown in Figure 4b and Figure 4c, the greater recycle flow rate leads to marked effects on the individual SDU and CVD reactor. An increased recycle flow rate leads to greater Sabatier conversion at a constant system inlet H_2:CO_2 due to the greater amount of excess H_2 that improves the reaction rate and shifts equilibrium toward the products (CH_4 and H_2O). The unreacted H_2 that flows through the SDU, however, leads to a significant detriment to the CVD reactor conversion due to its inhibitory effects on carbon deposition and dilution effects on the reactant residence time in the CVD reactor. As seen in both Figure 4b and Figure 4c, the sensitivity of the Sabatier and CVD conversion to the recycle flow rate is much greater at the higher recycle flow rates, which may exacerbate the need for very precise flow controllers for hardware testing if complete loop closure is desired. In general, if trying to maintain the H_2:CO_2 into the SDU between 4 and 4.5, a greater recycle flow rate appears to trend both the SDU and CVD reactor toward worsening performance (i.e., conversion) as indicated by the negative slope of the bounding green box in the figures below.

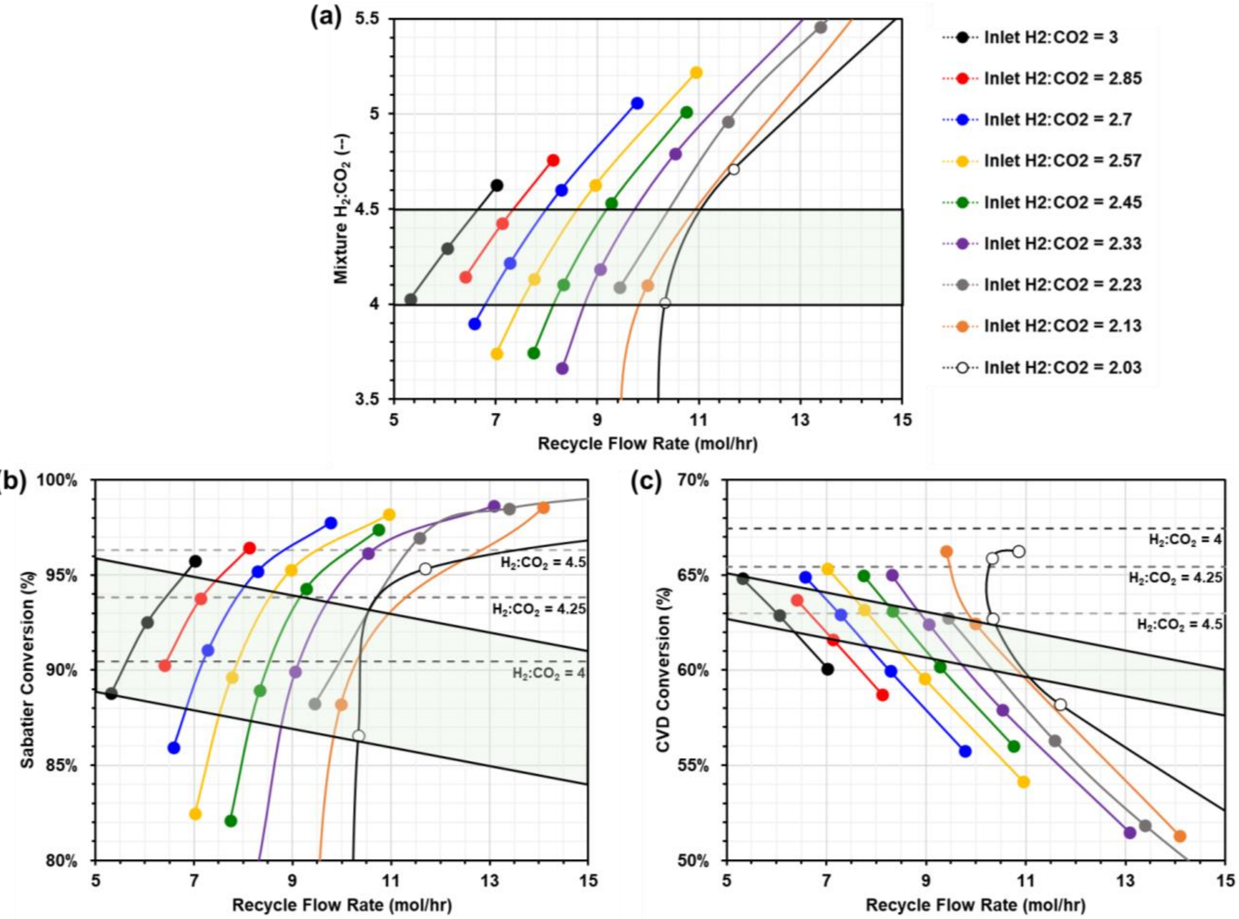

Figure 4. Plots of the (a) mixture H_2:CO_2, (b) Sabatier conversion, and (c) CVD conversion at different recycle flow rates and system inlet H_2:CO_2.

Figure 5 plots the mixture H_2O production rate from the SDU (Figure 5a), SDU O_2 recovery (Figure 5b), and system O_2 recovery (Figure 5c), which is defined by Equation 4, at different recycle flow rates. As with the prior figures, the open-loop configuration simulations at a H_2:CO_2 of 4, 4.25, and 4.5 are also plotted as points of comparison. The figures below are representative of the simulated integrated system performance.

Despite the worsening individual reactor performances demonstrated in Figure 4b and Figure 4c, the integrated system generates more H_2O, and is able to achieve greater O_2 recovery. The H_2O production increases because not only is H_2 being recovered from the SDU CH_4 byproduct via the CVD reactor effluent, but also unreacted CO_2 from the first pass of the SDU is being recycled and given more opportunities to reduce. The SDU O_2 recovery (Figure 5b) mirrors the H_2O production rate trends and shows a flattening around 97%. This is a significant improvement from the open-loop configuration, which achieved a SDU O_2 recovery of 91.6% at a H_2:CO_2 of 4.5.

The most significant effect of an increased recycle flow rate and decreased system inlet H_2:CO_2 is that the integrated system balance operates near the stoichiometry of water electrolysis and hence achieves a much greater system O_2 recovery compared to the open-loop simulations. The open-loop simulations predict a system O_2 recovery of 43.1% with a H_2:CO_2 of 4, whereas the integrated system was able to achieve a system O_2 recovery above 95%. Another result to note is that the system O_2 recovery is far more sensitive to the system inlet H_2:CO_2, whose decrease is facilitated by a higher recycle flow rate of the CVD effluent, rather than strictly increasing the recycle flow rate at a fixed system inlet H_2:CO_2. This result makes sense where the system O_2 recovery is mainly dictated by the difference between the system inlet H_2:CO_2 versus the output from a water electrolysis system (i.e., H_2:O_2 = 2). These results suggest that the integrated system is capable of operating together to achieve a high level of O_2 loop closure that may sustain long exploration missions with limited H_2 resupply. However, the reduction in the individual reactor performances is interesting and may suggest system modifications (e.g., intermediate H_2 separations to limit byproduct gas recycle) to improve performance.

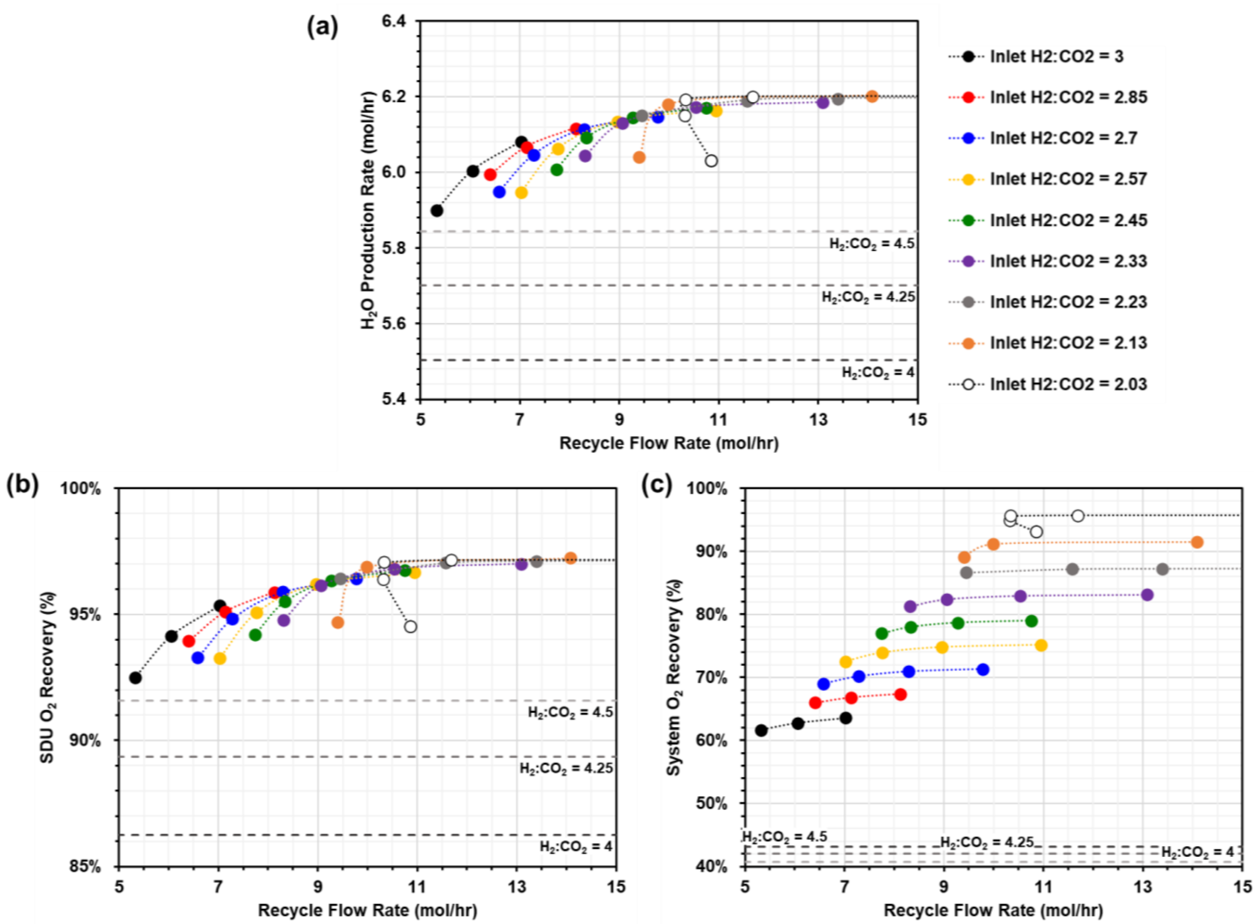

Figure 5. Plots of the (a) H_2O production rate, (b) SDU O_2 recovery, and (c) system O_2 recovery at different recycle flow rates and system inlet H_2:CO_2.

2. Transient Simulation Results

Transient simulations over a dynamic substrate (i.e., with carbon deposition) were performed with a recycle flow rate of 10.3 mol/hr and system inlet H_2:CO_2 of 2.03. These operating conditions represent one of the high-performing fresh substate simulation points that achieved approximately 95% system O_2 recovery. The transient simulation was run for 250 hr of simulation time. Figure 6 plots the CVD CH_4 conversion (Figure 6a), CVD effluent C_2H_2 mole fraction (Figure 6b), and CVD effluent composition (Figure 6c) versus the simulated time on stream. For their brassboard testing, Honeywell's stopping criteria that dictate when to end a run were (1) CH_4 conversion below 50%, (2) estimated density of any substrate layer exceeding 1.8 g/cm^3, or (3) C_2H_2 concentration in the CVD effluent greater than 1 mol%.[9] These criteria were established to provide sufficient H_2 to sustain the Sabatier reactor and to avoid risk of soot generation, which tends to be preceded by an increasing C_2H_2 concentration.

As shown in Figure 6a, the substrate starts at a lower CH_4 conversion in the integrated SDU and CVD reactor system (58.5%) compared to the standalone CVD reactor (68.5%) due to the excess H_2 and other byproducts that are fed along with CH_4 to the CVD reactor. The decreasing CH_4 conversion of the integrated system with time follows a similar trend as the standalone system but is offset by the difference in the initial conversion between the two configurations. The integrated system reaches the 50% CH_4 conversion stop criterion after approximately 110 hr compared to 275 hr for the standalone CVD reactor. Despite the uncertainty that may be present in the simulation (as will be discussed in Section IV.C), the results suggest an integrated system consisting of the Sabatier and CVD reactors will lead to a significant decrease in the maintenance interval, which is accompanied by an increase in the consumable substrate mass.

Furthermore, the integrated system shows higher C_2H_2 concentration in its CVD effluent compared to the standalone CVD reactor (Figure 6b), which appears to be commensurate with a rapidly increasing ethylene and C6+

concentrations (Figure 6c). The high concentration of C6+ species in the CVD effluent is indicative of soot precursor formation and suggests that operations past the 110 hr time on stream may produce a significant amount of the undesirable soot product that may be entrained within the gas stream. Thus, although system integration aids in achieving high system O_2 recovery (> 95%), it may also significantly reduce the maintenance interval and increase the necessary consumables mass for the system.

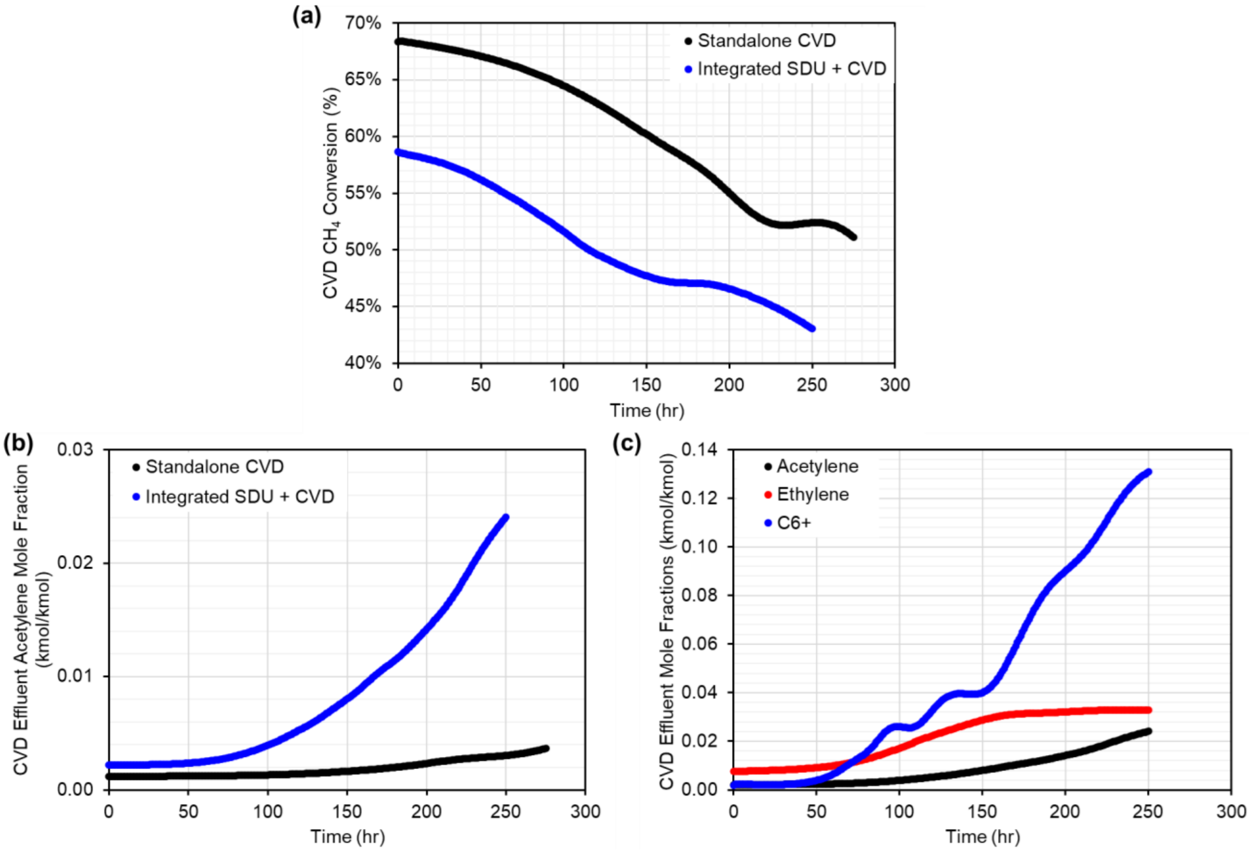

Figure 6. Plots of the (a) CH_4 conversion and (b) CVD effluent acetylene mole fraction versus time for the standalone and integrated systems as well as the (c) integrated system's CVD effluent composition versus time.

Figure 7 shows the integrated system O_2 recovery versus time. Interestingly, despite the significant reduction in the CVD reactor's CH_4 conversion and reaching the reactor stop criteria after 110 hr, the system O_2 recovery sees a much smaller reduction from 95.4% to 93.2%. After 250 hr, the system recovery decreases much more significantly to 85.3%. Therefore, within its operational bounds up until 110 hr, the simulation suggests that the integrated system is able to maintain a high level of performance. Thus, the major detriment of SDU and CVD reactor integration is the significant reduction in the maintenance interval.

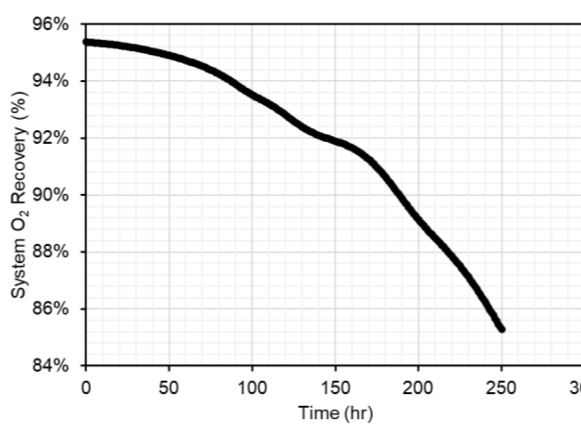

Figure 7. Integrated system O_2 recovery over time.

Next, Figure 8 provides insights into the some of the more specific tracked parameters within the simulation including the mixture H_2:CO_2 (Figure 8a) and recycle (or CVD effluent) composition of the CH_4, CO_2, and H_2 (Figure 8b). Immediately upon simulation start, the mixture H_2:CO_2 continuously decreases. The decrease in the mixture H_2:CO_2 is a result of the CVD reactor substrate dynamics. As the solid carbon deposits and densifies within the substrate, the CVD reactor conversion decreases, and hence, its H_2 generation rate also decreases. The lower H_2

generation rate reduces the $H_2:CO_2$ at the SDU inlet after mixing the system feed with the recycled CVD effluent. In the real system, if it is desired to maintain a constant mixture $H_2:CO_2$, then a supplemental H_2 will need to be fed that adjusts itself according to the recycle flow rate and composition. These simulation results indicate the potential need for a more sophisticated and precise flow control scheme.

The result of the lower mixture $H_2:CO_2$ into the SDU is reflected in the recycle (or CVD effluent) composition, which shows a decrease in the CH_4 and H_2 concentrations and a significant increase in the unreacted CO_2 concentration over time. Therefore, the simulations show how dynamics in one of the reactor systems can lead to intensified effects in the other reactor system that may worsen over time if left unchecked. The results from this analysis provide valuable insight into how operations of an integrated CO_2 system may differ from the expectations from standalone testing.

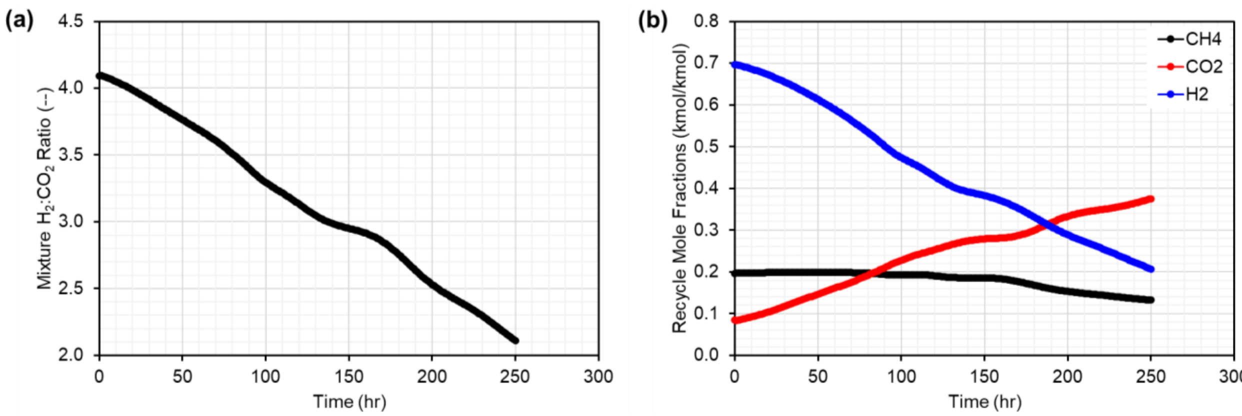

Figure 8. Plots of the (a) mixture $H_2:CO_2$, (b) recycle flow rate, and (c) recycle stream composition versus time for the integrated system.

C. Analysis Sources of Uncertainty

This analysis of the integrated Sabatier and CVD reactor is not without its sources of uncertainty, including the discrepancy between the model and brassboard reactor testing with regard to H_2 inhibition, the lack of byproduct reactions in the Sabatier reactor model, and the loosely heuristic nature of the stop criterion for the CVD reactor. This section intends to discuss these uncertainties and their expected effect on the quantitative accuracy of the analysis results. However, it is believed that the qualitative trends predicted by the models should hold.

As shown in Chen, *et al.* (2024), the CVD reactor model, which is based on literature kinetic parameters, differs from the brassboard CVD reactor testing in that it does include an inhibitory effect of H_2 on conversion, which was not observed during testing. H_2 inhibition was expected based on literature observations of carbon vapor infiltration systems where H_2 is believed to block the active sites for deposition.[19-22] However, the brassboard CVD reactor experiments showed no such H_2 inhibition effect. This difference between the CVD reactor model and brassboard CVD reactor may cause the CVD model to underpredict the CH_4 conversion as the H_2 concentration in the feed increases. Therefore, the model may predict reaching the stop criterion of a minimum CVD reactor conversion of 50% conversion sooner than reality. This would effectively cause underprediction of the maintenance interval and overprediction of the consumable substrate mass required.

Additionally, the Sabatier reactor model excludes the consideration of byproduct (e.g., C_2 hydrocarbons and larger) reactions since it only considers the CH_4 steam reforming and H_2O gas shift reactions. Some of the hydrocarbon byproducts of CH_4 pyrolysis may be consumed within the Sabatier reactor via steam reformation. Future updates to the integrated model will consider the C_2H_2 steam reforming reactions within the Sabatier reactor. However, the current model may underpredict H_2 production as a result of steam reformation of byproduct hydrocarbons (i.e., C_2H_2 and ethane), albeit in relatively small amounts (< 2 mol%), and overpredict accumulation of the major byproduct C_2H_2.

The last source of uncertainty for our conclusions is in the stop criterion (i.e., minimum 50% conversion for the CVD reactor). This criterion is based on a loose heuristic that too much CH_4 at the inlet to the Sabatier will prevent light off. However, there has been no experimental verification of this criterion. This 50% conversion criterion may be more thoroughly assessed for appropriateness and to understand the feasibility of operating at lower conversion. By being able to operate at below 50% conversion, the time interval between substrate changeout would increase. This additional consideration, however, does not affect the comparison between the standalone and integrated case made herein since both use the same stop criterion. Overall, these sources of uncertainty may suggest using these modeling results to elucidate qualitative trends in system performance.

V. Conclusion

In this work, a model of the integrated Sabatier (i.e., SDU) and CVD reactor systems was developed to assess the effects of system integration on their combined performance and compared to their standalone reactor performances. The integrated SDU and CVD reactor model development leveraged existing models of the individual SDU and CVD reactors. The use of modeling and simulation to support technology development by providing a priori insights into these hardware integrations is a powerful tool in that it is more flexible than testing real hardware, allows for rapid assessment of different operating conditions and configurations, and requires fewer resources to implement.

Simulation and analysis of the integrated SDU and CVD reactor system with fresh substrate at steady state showed that recycling the CVD effluent improves the system O_2 recovery, with > 95% O_2 recovery being achievable while reducing the necessary H_2:CO_2 into the system. However, the system integration leads to a detriment of the individual reactor performances with decreasing SDU and CVD reactor conversions as the recycle flow rate of CVD effluent increases. This reduction in individual reactor performance is, in part, due to the increased amount of byproducts and the dilution effects they impart on the reaction kinetics.

Transient simulation and analysis of the integrated SDU and CVD reactor system were used to show how the dynamically changing CVD reactor, whose substrate densifies over time due to the depositing carbon, leads to worsening system performance over time, with a reduction in the system O_2 recovery from 95.4% to 93.2% over 110 hr and a further reduction to 85.3% over 250 hr. Albeit, the system performance reduction is rather small, the larger effect on operations may come from a reduction in the maintenance interval of the integrated reactor system. The transient simulation showed the integrated system reached its below 50% CH_4 conversion stop criteria after 110 hr, which is a shorter maintenance interval compared to that from the standalone brassboard reactor testing. These simulation results suggest that, despite the sources of uncertainty, the integrated Sabatier and CVD reactor systems would lead to a shortening of the maintenance interval and hence an increase in the consumable substrate mass that would be needed on a long-duration exploration mission. The simulation results also indicate that the CVD reactor dynamics lead to decreasing H_2:CO_2 into the SDU for the closed-loop system, which may necessitate supplemental H_2 feed and a precise flow control system if it is desired to maintain a constant mixture H_2:CO_2 over the course of a run.

Note, however, that the integrated SDU and CVD model is not without its sources of uncertainty, which may skew the simulation results. In particular, some model aspects that may be updated to improve its fidelity include a more complete definition of the CO_2 and CO interconversions within the CVD reactor model, fine tuning the H_2 inhibition effects in the CVD reactor to achieve agreement between the model and brassboard reactor, expanding the Sabatier reactor's kinetic model to include some of the major byproducts (e.g., C_2H_2), and reconsideration or further assessment of the operational stop criterion for the system. Model advancement may also be supported by integrated Sabatier and CVD reactor testing where the test data can be used to improve the models in an iterative model development cycle. Despite these uncertainties, the integrated model of the SDU and CVD reactor system has provided valuable insight that may be beneficial for test planning and operations of the real-world counterparts.

Acknowledgments

The author would like to acknowledge and thank Tim Giesy and Kagan Crawford of NASA's Marshall Space Flight Center for their technical input throughout this work; Stephen F. Yates of Honeywell Aerospace for his technical insight into Honeywell's carbon vapor deposition reactor; Christian Junaedi of Precision Combustion, Inc. for his technical insight into their Sabatier development unit; and the Mars Campaign Office Exploration Life Support Systems project for their support of this work.

References

[1] Samplatsky, D. J., Grohs, K., Edeen, M., Crusan, J. and Burkey, R., "Development and Integration of the Flight Sabatier Assembly on the ISS, AIAA 2011-5151," in *41st International Conference on Environmental Systems*, Portland, Oregon, 17-21 July 2011.

[2] Yu, P., *et al*., "Poisoning Evaluation of On-Orbit Sabatier Assembly, ICES-2020-378," in *2020 International Conference on Environmental Systems*, 31 July 2020.

[3] Yu, P., *et al*., "“Getter” Development for International Space Station Sabatier Assembly, ICES-2022-54," in *51st International Conference on Environmental Systems*, St. Paul, Minnesota, 10-14 July 2022.

[4] Junaedi, C., Hawley, K., Walsh, D., Roychoudhury, S., Abney, M. B. and Perry, J. L., "Compact and Lightweight Sabatier Reactor for Carbon Dioxide Reduction, AIAA 2011-5033," in *41st International Conference on Environmental Systems*, Portland, Oregon, 17-21 July 2011.

[5] Junaedi, C., Hawley, K., Walsh, D., Roychoudhury, S., Abney, M. B. and Perry, J. L., "CO2 Reduction Assembly Prototype using Microlith-based Sabatier Reactor for Ground Demonstration, ICES-2014-090," in *44th International Conference on Environmental Systems*, Tucson, Arizona, 13-17 July 2014.

[6] Yates, S. F., Childers, A., Brom, N., Skomurski, S., Lo, C. and Abney, M. B., "Hydrogen Recovery by Methane Pyrolysis to Elemental Carbon, ICES-2019-103," in *49th International Conference on Envrionmental Systems*, Boston, Massachusetts, 7-11 July 2019.

[7] Childers, A., Yates, S. F., Brom, N. and Skomurski, S., "Chemical Vapor Deposition Methane Pyrolysis Enables Closed-Loop Oxygen Recovery: Reducing System Consumables, ICES-2021-33," in *50th International Conference on Environmental Systems*, Virtual, 12-15 July 2021.

[8] Childers, A., Yates, S. F., Parson, A., Smoke, J., Mehr, M. and Spencer, J., "Chemical Vapor Deposition Methane Pyrolysis Enables Closed-Loop Oxygen Recovery: Path to Flight, ICES-2022-390," in *51st International Conference on Environmental Systems*, St. Paul, Minnesota, 10-14 July 2022.

[9] Childers, A., Yates, S. F. and Triezenberg, M., "Methane Pyrolysis Enables Closed-loop Oxygen Recovery - Brassboard Evaluation, ICES-2023-88," in *52nd International Conference on Envrionmental Systems*, Calgary, Canada, 16-20 July 2023.

[10] Knox, J. C., "International Space Station Carbon Dioxide Removal Assembly Testing, 00ICES-234," in *30th International Conference on Environmental Systems*, Toulouse, France, 10-13 July 2000.

[11] Sherif, D. F. and Knox, J. C., "International Space Station Carbon Dioxide Removal Assembly (ISS CDRA) Concepts and Advancements, 2005-01-2892," in *35th International Conference on Environmental Systems*, Rome, Italy, 11 July 2005.

[12] Cmarik, G. E., Peters, W. T. and Knox, J. C., "4-Bed CO2 Scrubber – From Design to Build, ICES-2020-178," in *International Conference on Environmental Systems*, Virtual, 2020.

[13] Cmarik, G. E., Knox, J. C. and Garr, J., "Progress of Four Bed Carbon Dioxide Scrubber, ICES-2022-28," in *51st International Conference on Environmental Systems*, St. Paul, Minnesota, 10-14 July 2022.

[14] Knox, J. C., Cmarik, G. E. and Garr II, J. D., "Performance of the Four Bed Carbon Dioxide Scrubber ISS Technology Demonstration, ICES-2022-78," in *51st International Conference on Environmental Systems*, St. Paul, Minnesota, 10-14 July 2022.

[15] Knox, J. C., Cmarik, G. E. and Garr II, J. D., "Status of the Four Bed Carbon Dioxide Scrubber ISS Technology Demonstration 2022-2023," in *52nd International Conference on Environmental Systems*, Calgary, Canada, 16-20 July 2023.

[16] Shaw, L. A., "International Space Station as a Development Testbed for Advanced Environmental Control and Life Support Systems, ICES-2019-363," in *49th International Conference on Environmental Systems*, Boston, Massachusetts, 7-11 July 2019.

[17] Chen, T. T., Barta, D. J., Yates, S. F. and Triezenberg, M., "Kinetic Model Development of the Carbon Vapor Deposition Reactor to Predict Performance versus Design," in *53rd International Conference on Environmental Systems*, Louisville, Kentucky, 21-25 July 2024.

[18] Barrett, L. W., Sturtz, R. A. and Hutchinson, M. R., "Modeling of Gateway Environmental Control and Life Support Systems as a Means to Investigate the Subsystem and Integrated Architecture Performance, ICES-2023-305," in *52nd International Conference on Environmental Systems*, Calgary, Canada, 16-20 July 2023.

[19] Li, A., Norinaga, K., Zhang, W. and Deutschmann, O., "Modeling and simulation of materials synthesis: Chemical vapor deposition and infiltration of pyrolytic carbon," *Composites Science and Technology,* vol. 68, pp. 1097-1104, 2008.

[20] Becker, A. and Hüttinger, K. J., "Chemistry and Kinetics of Chemical Vapor Deposition of Pyrocarbon - IV Pyrocarbon Deposition from Methane in the Low Temperature Regime," *Carbon,* vol. 36, no. 3, pp. 213-224, 1998.

[21] Becker, A. and Hüttinger, K. J., "Chemistry and Kinetics of Chemical Vapor Deposition of Pyrocarbon - V Influence of Reactor Volume/Deposition Surface Area Ratio," *Carbon,* vol. 36, no. 3, pp. 225-232, 1998.

[22] Becker, A., Hu, Z. and Hüttinger, K. J., "A hydrogen inhibition model of carbon deposition from light hydrocarbons," *Fuel,* vol. 79, no. 13, pp. 1573-1580, 2000.